Resource and Power Allocation in SWIPT-Enabled Device-to-Device Communications Based on a Nonlinear Energy Harvesting Model

Haohang Yang, *Graduate Student Member, IEEE*, Yinghui Ye,
Xiaoli Chu, *Senior Member, IEEE*, and Mianxiong Dong, *Member, IEEE*

Abstract—Due to the limited battery capacity in mobile devices, simultaneous wireless information and power transfer (SWIPT) has been proposed as a promising solution to improve the energy efficiency (EE) in Internet-of-Things (IoT) networks, i.e., device-to-device (D2D) networks, by allowing mobile devices to harvest energy from ambient radio-frequency (RF) signals. However, the nonlinear behavior of RF energy harvesters has largely been ignored in the existing works on SWIPT. In this article, we propose to maximize the sum EE of all D2D links in a D2D underlaid cellular network by optimizing the resource and power allocation based on a nonlinear energy harvesting (EH) model. Toward this end, we first propose a prematching algorithm to divide the D2D links into a SWIPT-enabled group and a non-EH group that cannot meet the EH circuit sensitivity. We then develop a two-layer iterative algorithm to jointly optimize the D2D transmission power and the power splitting ratio to maximize the EE for each SWIPT-enabled D2D link. On this basis, we build the preference lists for both SWIPT-enabled D2D links and cellular user equipment (CUE), and propose a one-to-one constraint stable matching algorithm to maximize the sum EE of all SWIPT-enabled D2D links by optimizing the spectrum resource sharing between D2D links and CUEs. The sum EE of non-EH D2D links is maximized through an iterative power control algorithm and a one-to-one stable matching algorithm. Simulation results show that our proposed algorithms achieve a much higher sum EE than the existing matching-based energy-efficient resource allocation scheme for SWIPT-enabled D2D networks.

Index Terms—Device to device, energy efficiency (EE), energy harvesting (EH), matching theory, power control, resource allocation, simultaneous wireless information and power transfer (SWIPT), underlay.

I. Introduction

WITH the fast development of wireless communication systems, it is predicted that there will be seven trillion wireless devices worldwide by 2020 [1], imposing significant pressures on increasing the energy efficiency (EE) of Internet-of-Things (IoT) networks [2]–[4]. A large number of IoT applications are emerging in residential areas, hospitals, factories, etc. Several wireless techniques have been proposed to support IoT, such as ZigBee and WiFi. However, most of them work in unlicensed bands and cannot guarantee the Quality of Service (QoS) for IoT applications [5], [6]. It is expected that future IoT systems will mainly be supported by 5G mobile networks [7].

Meanwhile, machine-to-machine or device-to-device (D2D) communications are intrinsic to IoT systems. Hence, D2D communications underlaying cellular networks have been considered as a promising technology to support IoT networks [5], [6]. D2D communications, one of the important scenarios in IoT networks, allow two user equipment (UE) in proximity to communicate with each other directly without passing through a base station (BS) by reusing the spectrum resource of cellular links, and hence improve the EE of a cellular network. However, there will be mutual interference between spectrum-sharing D2D links and cellular UE (CUEs), which need to be mitigated through proper resource allocation schemes [8]–[10]. Meanwhile, radio-frequency (RF)-enabled energy harvesting (EH), which allows UE to harvest energy from ambient RF signals [11], has been proposed to improve the EE of wireless communications. One popular EH technology is the simultaneous wireless information and power transfer (SWIPT), where the receiver is able to harvest energy and process information simultaneously via a power splitting scheme or a time switching scheme [12]–[16]. In addition to WPT, techniques for EH from natural resources have also been developed for IoT networks [17]–[19].

The EE definition is based on the whole D2D link which comprises the energy harvested by the D2D receiver. Also, in the long term, each D2D user statically has the same probability of being a transmitter or a receiver, and the proposed algorithms will benefit all D2D users in the network. Although there is a considerable number of works on the D2D networks with EH, the researches on the SWIPT-based D2D are still insufficient due to the following reasons. Some works assume that the energy source is from the unstable

natural resource [20], e.g., solar energy. The other works allow the energy harvester to harvest energy from ambient RF signals [21]. SWIPT is not considered in both cases. Note that SWIPT is expected to operate under short distances because it is mainly limited by the received signal power and the minimum required energy for activating the EH circuit, also known as, the EH circuit sensitivity (e.g., -20 dBm [22], which is much higher than the thermal noise power), while the information transfer depends on the receive signal-to-interference-plus-noise ratio (SINR). The shared short-range nature between D2D communications and SWIPT motivates the combination of them to further improve the EE performance. For long-distance wireless transmissions in IoT networks, EH could employ laser charging, e.g., UAV-enabled IoT networks with laser charging were studied in [23] and [24].

The resource allocation schemes for conventional D2D communications without SWIPT may not be applicable for SWIPT-enabled D2D communications, where the conventionally considered harmful interference could be exploited for EH. Huang *et al.* [25] employed game theory to define the utility of SWIPT-enabled D2D links and allocated D2D transmission power by an iterative algorithm. In [11], a stable matching algorithm was proposed to optimize the spectrum resource and power allocation to improve the average EE for SWIPT-enabled D2D communications. In [26], a transmission flow mechanism was developed to evaluate the impact of different network parameters on the harvested energy and the outage capacity in a SWIPT-based D2D cooperative network. Lim *et al.* [27] proposed a scheme that selects between full duration (FD) and partial duration (PD) SWIPT schemes to maximize the data rate of a SWIPT-enabled D2D link. In [28], a power control scheme was proposed to maximize the D2D rate without degrading the performance of CUEs in a downlink SWIPT network.

However, the above works have assumed a simplified linear EH model, where the amount of harvested energy is linearly proportional to the received power, which is not the case in a practical EH system due to the nonlinearity of the diodes, inductors, and capacitors [29]. Moreover, the energy conversion efficiency was assumed a fixed value in [11], [21], [22], [25], and [26], while the power splitting ratio was assumed as a fixed value in [11] and [25]–[27], thus missing the opportunity to optimize it for improving the EE of a SWIPT-enabled D2D underlaid network.

In this article, we aim to maximize the sum EE of all D2D links in a SWIPT-enabled D2D underlaid cellular network, where D2D links reuse uplink resources and a piecewise linear EH model[1] is considered for SWIPT. Our main contributions are summarized as follows.

1) Considering the impact of EH circuit sensitivity, we propose a prematching algorithm to identify the D2D links that can perform SWIPT under the constraints of EH circuit sensitivity and minimum throughput requirement.

Based on the prematching results, we maximize the EE of each SWIPT-enabled D2D link.

2) We propose a one-to-one constraint stable matching algorithm to maximize the sum EE of SWIPT-enabled D2D links by optimizing the spectrum resource sharing between D2D links and uplink CUEs. This matching algorithm ensures that each SWIPT-enabled D2D link is matched to a CUE.

3) In the one-to-one constraint stable matching algorithm, the preference lists for both D2D links and CUEs are constructed based on the solutions to the per-D2D-link EE maximization problems, which jointly optimize the D2D transmission power and the power splitting ratio based on a piecewise linear EH model for each SWIPT-enabled D2D link. Since the two variables are coupled in the objective function, making it difficult to solve, we propose a two-layer energy-efficient iterative algorithm (TLEEIA) to solve it by applying the block coordinated descent (BCD) method.

4) The sum EE of non-EH D2D links is maximized by devising an iterative power control algorithm and a stable matching algorithm but with lower complexity than that for SWIPT-enabled D2D links.

5) We perform extensive simulations to evaluate the EE performance of our proposed algorithms in comparison with a baseline scheme which employs our proposed algorithms based on a linear EH model, the matching-based energy-efficient resource allocation scheme in [11], and two heuristic algorithms, including proposed matching with maximum D2D transmission power scheme and random matching with maximum D2D transmission power scheme. The impacts of some system parameters, e.g., the number of D2D links or CUEs and the D2D communication range, on the sum EE of D2D links are also examined.

The remainder of this article is organized as follows. The system model of a D2D communication underlaid cellular network is built in Section II. In Section III, the detailed EE optimization process for each SWIPT-enabled D2D link is introduced. In Section IV, a one-to-one constraint stable matching algorithm is proposed to solve the resource allocation problem so as to maximize the sum EE of SWIPT-enabled D2D links, the sum EE maximization of non-EH D2D links is also derived in this section. Section V analyzes the computational complexity of our proposed algorithms. In Section VI, the simulation results are presented. Section VII concludes this article.

II. System Model

A. Network Model

As shown in Fig. 1, a BS[2] is located at the center of a signal cell that covers CUEs and D2D users. Each D2D link i consists of transmitter i (TX i) and receiver i (RX i), and

---

[1]There are many nonlinear EH models reported in the literature. The piecewise linear EH model is one of the most analytically tractable models while ensuring a good accuracy [30].

[2]The BS obtains all the necessary channel state information (CSI) by collecting feedback from the CUEs and D2D devices. In LTE/LTE-A networks, each user (which can be a CUE or a BS assisted D2D device) is scheduled to periodically send measurement reports (including CSI) to the serving BS [31], while the acquisition and reporting of CSI between D2D/cellular transmitters and D2D receivers could employ the techniques proposed in [31] and [32].
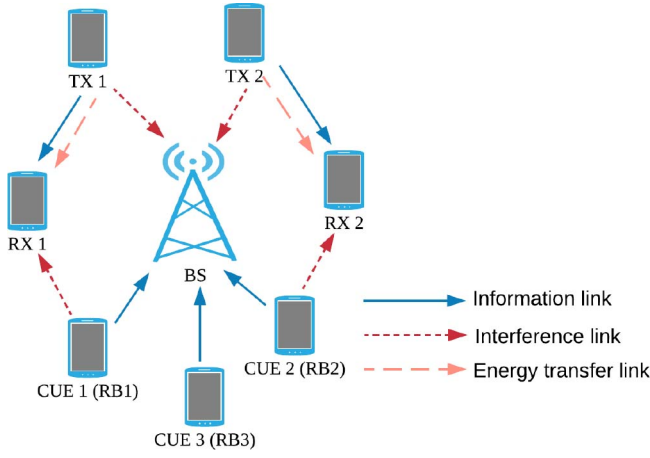
Fig. 1. SWIPT-enabled D2D networks.

Fig. 2. Power splitting unit.

they communicate with each other directly by sharing the spectrum resource with a CUE in an underlaid mode.[3] We assume that there are M orthogonal resource blocks (RBs) allocated to M CUEs and shared by N D2D links. For simplicity, we denote all CUEs and all D2D links by the sets $\hat{C} = \{1, 2, \ldots, k, \ldots, M\}$ and $\hat{D} = \{1, 2, \ldots, i, \ldots, N\}$, respectively. We suppose that $N \leq M$ and that a D2D link can only share the RB of one CUE and the RB of a CUE can only be reused by at most one D2D link.[4] For simplicity, the entire time block is normalized to 1. A flat fading channel is considered, where the distance-dependent pathloss and Rayleigh fading are used to model the large-scale fading and the small-scale fading, respectively. It is also assumed that the channel state remains static within each RB. There is no intracell interference among CUEs by employing orthogonal frequency-division multiple access (OFDMA) [36], [37]. Besides, QoS in this article is measured by the SINR.

We assume that D2D peer discovery and link establishment have been completed. As a D2D pair reuses an uplink RB of a CUE, the D2D receiver receives interference from the co-channel CUE while the D2D transmitter causing interference to the BS. We assume that each D2D device is equipped with an RF EH circuit and an information decoding unit. Due to the EH circuit sensitivity and D2D link QoS requirement, some D2D links cannot perform SWIPT. Thus, we will propose a prematching algorithm to divide all D2D links into non-EH D2D links and SWIPT-enabled D2D links in Section III.

B. Non-EH D2D Links

As discussed in Section II-A, in the D2D underlaid cellular network, the interference to the BS comes from a co-channel D2D transmitter and only a co-channel CUE causes interference to a D2D receiver. Thus, when sharing the same RB, the SINR of cellular link k[5] and non-EH D2D link i are given by

$$
\begin{aligned}
\text{SINR}_k^C &= \frac{P_k^C h_k^C}{P_i^D h_i^B + N_0 + N_1} \\
&= \frac{P_k^C d_k^{C-\alpha} h_k'^C}{P_i^D d_i^B h_i'^{B'} + N_0 + N_1}
\end{aligned}
\tag{1}
$$

$$
\begin{aligned}
\text{SINR}_i^D &= \frac{P_i^D h_i^D}{P_k^C h_{k,i} + N_0 + N_1} \\
&= \frac{P_i^D d_i^{D-\alpha} h_i'^D}{P_k^C d_{k,i}^{-\alpha} h_{k,i}' + N_0 + N_1}
\end{aligned}
\tag{2}
$$

where P_k^C and P_i^D are the transmission power[6] of CUE k and D2D transmitter i, respectively, h_k^C and h_i^D represent the channel responses of cellular uplink k and D2D link i, respectively, d_k^C is the distance from CUE k to the BS, and d_i^D represents the distance between the TX and RX of D2D link i. Similarly, h_i^B and $h_{k,i}$ are the channel responses of interference link from D2D link i to BS and the interference link from CUE k to D2D link i, respectively, d_i^B and $d_{k,i}$ are the distance of the interference links above, $h_k'^C$, $h_i'^D$, $h_i'^B$, and $h_{k,i}'$ are the Rayleigh channel coefficients accordingly, α is the free space pathloss exponent, N_0 is the additive white Gaussian noise (AWGN) power, and N_1 is the noise power due to RF band to base band conversion.

Then, the throughputs of cellular link k and D2D link i are, respectively, given by

$$
T_k'^C = \log_2\left(1 + \text{SINR}_k^C\right) \tag{3}
$$

$$
T_i'^D = \log_2\left(1 + \text{SINR}_i^D\right). \tag{4}
$$

C. SWIPT-Enabled D2D Links

SWIPT can be implemented in either a power splitting mode or a time switching mode. We consider the power splitting mode in this article since it has been proved to be more efficient in both throughput and EE [39]. As shown in Fig. 2, the power splitting unit splits the received radio signal into two signal streams. One stream is for information decoding

---

[3]Our proposed system will not introduce extra system overhead, the CSI estimation required in our proposed system is the same as that required in D2D networks without EH. As the optimization problem is solved at the BS for all the D2D links within its coverage, solving the optimization problem does not consume power at the D2D devices. In addition, the D2D receiver is able to harvest energy from the signals transmitted by the D2D transmitter and the co-channel CUE [21], [33].

[4]Multiple co-channel D2D links may experience strong mutual interference that needs to be mitigated by an advanced interference mitigation scheme. For analytical tractability, we assume that one RB is reused by at most one D2D link [11], [34], [35]. The case with multiple co-channel D2D links will be studied in our future work.
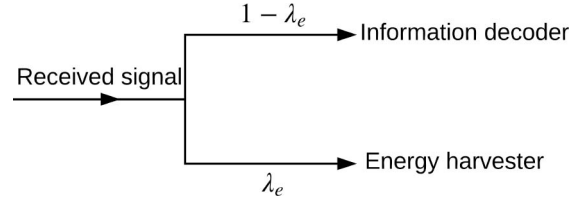
[5]Since most notations in this article are related to CUE k, but the optimization problem focuses mainly on maximizing the EE for D2D links, for notational simplicity, we will omit subscript k from notations where appropriate.

[6]For analytical tractability, we assume that all CUEs transmit at the maximum power level [11], [38]. The impact of CUE transmission power on the sum EE of D2D links will be evaluated through simulation in Section VI-D.

and the other is for EH, where λ_e denotes the power splitting ratio, which determines the portion of the received signal used for EH. Without loss of generality, we assume that the D2D receivers are relatively far away from the BS so that the received power from the BS may fall below the EH circuit sensitivity. In this case, we do not consider EH from the BS, and a D2D receiver can harvest energy from the signals transmitted by its paired D2D transmitter and the interference from the co-channel CUE and the surrounding thermal noise.

For SWIPT-enabled D2D link i, the throughput is given by

$$T_i^D = \log_2\left(1 + \frac{(1 - \lambda_i^e)P_i^D h_i^D}{(1 - \lambda_i^e)(P_k^C h_{k,i} + N_0) + N_1}\right) \quad (5)$$

where the useful information signal, the interference, and the noise are scaled by the factor of $(1 - \lambda_i^e)$.

The received power for EH at D2D receiver i when sharing the RB with CUE k is given by

$$P_i^R = \lambda_i^e\left(P_i^D h_i^D + P_k^C h_{k,i} + N_0\right). \quad (6)$$

We employ the piecewise linear EH model proposed in [24], which fits over real measurement data. Accordingly, the amount of power harvested by D2D receiver i is given as

$$\text{EH}_i^D = \begin{cases} 0, & P_i^R \in \left[P_{th}^0, P_{th}^1\right] \\ k_j P_i^R + b_j, & P_i^R \in [P_{th}^j, \ P_{th}^{j+1}], \quad j \in 1, \ldots, L-1 \\ P_{\max}^{\text{EH}}, & P_i^R \in \left[P_{th}^L, P_{th}^{L+1}\right] \end{cases} \quad (7)$$

where $\mathbf{P_{th}} = \{P_{th}^j | 1 \le j \le L+1\}$ is the set of thresholds on P_i^R for $L + 1$ linear segments; k_j and b_j are the coefficient and the intercept of the linear function in the jth segment, respectively, P_{th}^1 denotes the minimum received power requirement for activating the RF EH circuit, and $P_{\max}^{\text{EH}}$ represents the maximum power the RF EH circuit can harvest. It has been shown in [40] and [41] that the piecewise linear EH model captures the harvested power more accurately than the linear EH model, the accuracy of the piecewise linear EH model improves with more segments, and a 4-piecewise linear EH model offers a good tradeoff between accuracy and computational complexity.

The total energy consumption of D2D link i is given as

$$\text{EC}_i^D = P_i^D + 2P_{\text{cir}} - \text{EH}_i^D \quad (8)$$

where P_{cir} is the circuit power consumption for a D2D transmitter (or a D2D receiver), including the power consumption of mixer, frequency synthesizer, etc.

III. PER-D2D-LINK ENERGY EFFICIENCY MAXIMIZATION FOR SWIPT-ENABLED D2D LINKS

In this section, we first propose a prematching algorithm to separate SWIPT-enabled D2D links and non-EH D2D links, then we maximize the EE of each potential SWIPT-enabled D2D link based on the prematching results.

Algorithm 1 Prematching Algorithm

Input: $\hat{D}, \hat{C}, P_k^C, P_{th}^1, \text{P}_{\max}, \text{T}_{\min}^{\text{D}}$.
Output: S_i^D, Inf^D, Eha^D.
Initialize: $S_i^D = \hat{C}, Inf^D = \emptyset, Eha^D = \emptyset$.
1: **for** $i \in \hat{D}$ **do**
2:     **for** $k \in \hat{C}$ **do**
3:         obtain $\lambda_{i,min}^e$ using (9), obtain $T_{i,max}^D$ using (10).
4:         **if** $\lambda_{i,min}^e > 1$ or $T_{i,max}^D \le \text{T}_{\min}^{\text{D}}$ **then**
5:             $S_i^D \backslash k$.
6:         **end if**
7:     **end for**
8:     **if** $S_i^D = \emptyset$ **then**
9:         $Inf^D \cap i$.
10:     **else**
11:         $S_i^D \ne \emptyset, Eha^D \cap i$.
12:     **end if**
13: **end for**

A. Prematching Algorithm

Considering the EH circuit sensitivity, we divide the D2D links into two groups: one group denoted by Eha^D for SWIPT-enabled D2D links (which can activate the EH circuit at the receiver while meeting the minimum D2D throughput requirement) and the other denoted by Inf^D for non-EH D2D links (which cannot perform SWIPT). We propose a prematching algorithm in Algorithm 1 to obtain the two groups. For any D2D link i, the partner selection set S_i^D is initialized as $\hat{C}$. If when reusing the RB of CUE k, and transmitting at the maximum transmission power $P_{\max}$, D2D link i cannot meet the EH circuit sensitivity and/or the D2D throughput requirement, then CUE k is removed from S_i^D. This step is repeated for each CUE in the set $\hat{C}$ and the partner selection sets S_i^D for D2D link i are obtained, the minimum power splitting ratio for meeting the EH circuit sensitivity requirement of D2D link i is calculated as

$$\lambda_{\min}^{e,i} = \frac{P_{th}^1}{P_{\max}h_i^D + P_k^C h_{k,i} + N_0}. \quad (9)$$

As $\lambda_{i,\min}^e$ cannot exceed 1, we can obtain the maximum throughput of D2D link i when satisfying the EH circuit sensitivity requirement as

$$T_{i,\max}^D = \log_2\left(1 + \frac{P_{\max}h_i^D}{P_k^C h_{k,i} + N_0 + \frac{N_1}{1-\lambda_{i,\min}^e}}\right). \quad (10)$$

The above procedures will be performed for each D2D link to obtain their partner selection set. At the end of Algorithm 1, if the partner selection set for a D2D link is empty, then this D2D link is grouped into the set Inf^D; otherwise, it is grouped into the set Eha^D.

B. Per-D2D-Link EE Problem Formulation

The partner selection set (returned by Algorithm 1) for a SWIPT-enabled D2D link may contain more than on CUE, while a CUE may appear in more than one partner selection set. In order to optimize the matching between SWIPT-enabled

D2D links and CUEs so that the sum EE of SWIPT-enabled D2D links is maximized, we first maximize the EE for each SWIPT-enabled D2D link i in Eha^D. The EE is defined as the ratio of throughput T_i^D to the total power consumption EC_i^D [10].

The EE of D2D link i in Eha^D when reusing the RB allocated to CUE k in S_i^D is given by

$$EE_i^D = \frac{T_i^D}{EC_i^D} = \frac{\log_2\left(1 + \frac{P_i^D h_i^D}{(P_k^C h_{k,i} + N_0) + \frac{N_1}{(1-\lambda_i^e)}}\right)}{P_i^D + 2P_{cir} - EH_i^D}. \quad (11)$$

Accordingly, the EE maximization problem of SWIPT-enabled D2D link i is formulated as

P1: $\displaystyle\max_{\{P_i^D, \lambda_e^i, i \in Eha^D\}} EE_i^D$

$$\begin{aligned}
\text{s.t.} \quad & C1: 0 < P_i^D \le P_{max} \\
& C2: 0 \le \lambda_i^e \le 1 \\
& C3: T_i^D \ge T_{min}^D \\
& C4: T_k^C \ge T_{min}^C \\
& C5: P_i^R \ge P_{th}^1 \\
& C6: P_{th}^j \le P_i^R \le P_{th}^{j+1}, \quad j \in 0, \dots, L \quad (12)
\end{aligned}$$

where C1 denotes the maximum transmission power for all D2D transmitters; C2 sets the range of the power splitting ratio; C3 and C4 set the minimum throughput requirement for D2D links and cellular links, respectively; C5 denotes the minimum received power required for a D2D receiver to activate its EH circuit, i.e., the EH circuit sensitivity; and C6 indicates that the energy harvester of D2D receiver i works in the jth linear segment in the piecewise linear EH model.

In order to solve **P1**, we propose a TLEEIA, which includes an outer loop algorithm given in Algorithm 2 and an inner loop iterative algorithm given in Algorithm 3. In Algorithm 3, the maximum number of segments N_{max} in the piecewise linear EH model that P_i^R belongs to is obtained by calculating $P_{i,max}^R = P_{max} h_i^D + P_k^C h_{k,i} + N_0$ and comparing the calculated value with the piecewise linear EH model in (7), where $P_{i,max}^R$ is the maximum received power of D2D RX i. Then, Algorithm 3 continues to calculate the optimal values of $\{P_{i,1}^D, \dots, P_{i,j}^D, \dots, P_{i,N_{max}}^D\}$, $\{\lambda_{i,1}^e, \dots, \lambda_{i,j}^e, \dots, \lambda_{i,N_{max}}^e\}$, and $\{EE_{i,1}^D, \dots, EE_{i,j}^D, \dots, EE_{i,N_{max}}^D\}$ that maximize the EE of SWIPT-enabled D2D link i when it is matched with every possible CUE in the jth segment. In Algorithm 2, the optimal segment that maximizes the EE of SWIPT-enabled D2D link i when matched with every possible CUE is determined by $j^* = \arg\max_j\{EE_{i,1}^D, \dots, EE_{i,j}^D, \dots, EE_{i,N_{max}}^D\}$, and the corresponding optimal λ_i^{e*}, P_i^{D*}, and EE_i^{D*} are obtained.

C. Inner Loop Iterative Algorithm

Since **P1** is a nonconvex fractional programming problem and difficult to solve, we transform it into a nonfractional problem by employing nonlinear fractional programming [42], given by

P2: $\displaystyle\max_{\{P_i^D, \lambda_i^e\}} T_i^D - Q_i^D EC_i^D, \quad i \in Eha^D$

$$\text{s.t.} \quad C1{-}C6 \quad (13)$$

Algorithm 2 TLEEIA—Outer Loop Algorithm

Input: Eha^D, S_i^D, $\lambda_{i,j}^e$, $P_{i,j}^D$, $EE_{i,j}^D$
Output: P_i^{D*}, λ_j^{e*}, EE_i^{D*}.
1: **for** $i \in Eha^D$ **do**
2:    **for** $k \in S_i^D$ **do**
3:       **for** $j = 1 : N_{max}$ **do**
4:          $j^* = \arg\max_j\{EE_{i,1}^D, \dots, EE_{i,j}^D, \dots, EE_{i,N_{max}}^D\}$.
5:          Obtain $P_i^{D*} = P_{i,j^*}^D$, $\lambda_i^{e*} = \lambda_{i,j^*}^e$, $EE_i^{D*} = EE_{i,j^*}^D$.
6:    **end for**
7:    **end for**
8: **end for**

---

where $Q_i^D = EE_i^D$. Based on [42], we have the following theorem for solving **P2**.

Theorem 1: The optimal Q_i^{D*} can be achieved if and only if $T_i^{D*} - Q_i^{D*}EC_i^{D*} = 0$, where $Q_i^{D*} = \max_{\{P_{i,D^*}\}} EE_i^D = (T_i^{D*}/EC_i^{D*})$, which is the maximum EE of D2D link i, and P_i^{D*}, T_i^{D*}, and EC_i^{D*} are the corresponding optimal values when D2D link i reuses the RB of CUE k.

According to Theorem 1, we can address the original non-convex problem by solving **P2**. Q_i^D is regarded as the negative weight of EC_i^D and we set the initial value of Q_i^D as a small positive value.

We employ Lagrange dual decomposition and Karush–Kuhn–Tucker (KKT) conditions to solve **P2**. The Lagrange function is given by

$$\begin{aligned}
L(P_i^D, \lambda_i^e, \alpha, \beta, \gamma, \delta, \epsilon) = {} & T_i^D - Q_i^D EC_i^D \\
& - \alpha(P_i^D - P_{max}) - \beta(\lambda_i^e - 1) \\
& + \gamma(T_i^D - T_{min}^D) + \delta(T_i^C - T_{min}^C) \\
& + \epsilon(P_i^R - P_{th}^1)
\end{aligned} \quad (14)$$

where α, β, γ, δ, and ζ are the Lagrange multipliers for C1–C5, respectively. Then, the Lagrange dual optimization problem is obtained as

P3: $\displaystyle\min_{\{\alpha, \beta, \gamma, \delta, \epsilon \ge 0\}} \max_{\{P_i^D, \lambda_i^e\}} L(P_i^D, \lambda_i^e, \alpha, \beta, \gamma, \delta, \epsilon), \quad i \in Eha^D$

$$\text{s.t.} \quad C6. \quad (15)$$

To solve P3, we have the following proposition.

Proposition 1: **P3** is convex with respect to λ_i^e when we fix P_i^D and it is also convex with respect to P_i^D when we fix λ_i^e.

Proof: See Appendix A. ∎

Based on Proposition 1, we can find the locally optimal λ_i^e for a given P_i^D and the locally optimal P_i^D for the optimized λ_i^e by applying the BCD method.[7] Then, we use the KKT conditions to obtain the expression of λ_i^e for a fixed P_i^D by solving the following equation:

$$\frac{\partial L(P_i^D, \lambda_i^e, \alpha, \beta, \gamma, \delta, \epsilon)}{\partial \lambda_i^e} = 0. \quad (16)$$

---

[7]Although the convergence of the BCD method cannot be analyzed theoretically [43], it can converge typically in a few iterations for a moderate number of users as shown in the simulation results.

Theorem 2: By solving (16) for λ_i^e, the optimal value of λ_i^e in **P3** is given as

$$\lambda_i^{e*} = \left\{ \frac{-a_2 \pm \sqrt{a_2^2 - 4a_1 a_3}}{2a_1} \right\}^+ \tag{17}$$

where $\{X\}^+ = \max\{0, X\}$, $a_1 = K(GH + H^2)$, $a_2 = K(G + 2H)N_1$, $a_3 = KN_1^2 - J$, $G = P_i^D h_i^D$, $H = P_k^C h_{k,i} + N_0$, $K = \beta + (Q_i^D + \epsilon)k_j(G + H)$, and $J = GN_1 \log_2^e(1 + \gamma)$.

Proof: See Appendix B. ∎

Similarly, when λ_i^e is fixed, the optimal value of P_i^D can be obtained by solving the following equation:

$$\frac{\partial L(P_i^D, \lambda_i^e, \alpha, \beta, \gamma, \delta, \epsilon)}{\partial P_i^D} = 0. \tag{18}$$

Theorem 3: By solving (18) for P_i^D, the optimal value of P_i^D can be obtained in a closed form as

$$P_i^{D*} = \max\{0, P_1\} \tag{19}$$

with

$$P_1 = \begin{cases} X_N + \sqrt[3]{\frac{-y_N + \sqrt{y_N^2 - g^2}}{2a_1}} + \sqrt[3]{\frac{-y_N - \sqrt{y_N^2 - g^2}}{2a_1}}, & y_N^2 > g^2 \\ X_N - \theta, X_N + 2\theta, & y_N^2 = g^2 \\ X_N + 2\theta \cos\left(\phi - \frac{2\pi n}{3}\right), \quad [n = 0, 1, 2]. & y_N^2 < g^2 \end{cases} \tag{20}$$

where $b_1 = m_3 h_i^D h_{i,B}^2$, $b_2 = (2m_3 m_5 + m_3 m_6)h_i^D h_i^B - (m_1 - m_2 m_3)h_{i,B}^2$, $b_3 = (m_3 m_5^2 + m_3 m_5 m_6 + m_4)h_i^D - (2m_1 m_5 + m_1 m_6 - 2m_2 m_3 m_5 - m_2 m_3 m_6)h_{i,B}$, $b_4 = m_2 m_4 + m_2 m_3 m_5^2 + m_2 m_3 m_5 m_6 - m_1 m_5^2 - m_1 m_5 m_6$. $X_N = (-m_2/3m_1)$, $y_N = (2b_3^3/27b_1^2) - [(b_2 b_3)/3b_1] + b_4$, $g = 2b_1 \sqrt{[(b_2^2 - 3b_1 b_3)/9b_1^2]^3}$, $\phi = (1/3)arc\cos(-y_N/g)$, $\theta^2 = [(m_2^2 - 3m_1 m_3)/9m_1^2]$, $m_1 = (1 + \gamma)h_i^D \log_2^e$, $m_2 = P_k^C h_{k,i} + N_0 + [N_1/(1 - \lambda_i^e)]$, $m_3 = Q_i^D(1 + (1 - \lambda_i^e)\eta h_i^D - k_j h_i^D) + \alpha - \epsilon\lambda_i^e k_j h_i^D$, $m_4 = P_k^C h_k^C h_i^B \log_2^e \delta$, $m_5 = N_0 + N_1$, $m_6 = P_k^C h_k^C$, and the sign of θ is the same as that of $\sqrt[3]{(y_n/2b_1)}$.

Proof: See Appendix C. ∎

Then, we use the gradient method to update the values of the Lagrange multipliers as follows:

$$\alpha = \{\alpha + s_1(P_i^D - P_{\max})\}^+ \tag{21}$$

$$\beta = \{\beta + s_2(\lambda_i^e - 1)\}^+ \tag{22}$$

$$\gamma = \{\gamma - s_3(T_i^D - T_{\min}^D)\}^+ \tag{23}$$

$$\delta = \{\delta - s_4(T_k^C - T_{\min}^C)\}^+ \tag{24}$$

$$\epsilon = \{\epsilon - s_5(P_i^R - P_{th}^1)\}^+ \tag{25}$$

where s_1, s_2, s_3, s_4, and s_5 are the step sizes of the associated constraints and they need to be properly initialized for guaranteeing the convergence and optimality. The step size is usually based on the objective function and simulation parameters, we set the step size for updating the five Lagrange multipliers as 10^{-5} in this article.

We propose an inner loop iterative algorithm in Algorithm 3 to obtain the optimal value of $\lambda_{i,j}^e$, $P_{i,j}^D$, and $EE_{i,j}^D$ for each

---

Algorithm 3 TLEEIA—Inner Loop Iterative Algorithm

Require: Eha^D, S_i^D.
Output: $\lambda_{i,j}^e$, $P_{i,j}^D$, $EE_{i,j}^D$.
Initialize: $Q_i^D(t) = Q_i^D(0)$, $P_i^D(t) = P_i^D(0)$, I, ψ, $t = 0$.
1: Obtain $P_{i,R}^{max}$ and decide the maximum number of segments: N_{max}.
2: **for** $i \in Eha^D$ **do**
3:     **for** $k \in S_i^D$ **do**
4:         **for** $j = 1 : N_{max}$ **do**
5:             We use the initialization value $P_i^D(0)$ to obtain $\lambda_i^e(t)$ by calculating (17).
6:             **while** $t < I$ **do**
7:                 We use the achieved value of $\lambda_i^e(t)$ to obtain $P_i^D(t + 1)$ by calculating (20).
8:                 We use the calculated value of $P_i^D(t + 1)$ to obtain $\lambda_i^e(t + 1)$ by calculating (17).
9:                 **if** $T_i^D[\lambda_i^e(t + 1), P_i^D(t + 1)] - Q_i^D(t)EC_i^D[\lambda_i^e(t + 1), P_i^D(t + 1)] > \psi$ **then**
10:                    $Q_i^D(t + 1) = T_i^D[\lambda_i^e(t + 1), P_i^D(t + 1)]/EC_i^D[\lambda_i^e(t + 1), P_i^D(t + 1)]$.
11:                    **Update** Lagrange multipliers using (21)-(25).
12:                    **Continue**
13:                 **else**
                   $P_{i,j}^D = P_i^D(t + 1)$, $\lambda_{i,j}^e = \lambda_i^e(t + 1)$, $EE_{i,D}^j = Q_i^D(t)$.
14:                 **end if**
15:                 $t = t + 1$.
16:             **end while**
17:         **end for**
18:     **end for**
19: **end for**

SWIPT-enabled D2D link in the jth segment of the linear piecewise EH model. In Algorithm 3, t is the number of iteration step; and I denotes the maximum allowed number of iteration. The iteration terminates when the difference between the value of achieved EE and that of EE in the previous step is smaller than ψ or I is achieved.

IV. SUM ENERGY EFFICIENCY MAXIMIZATION

In this section, we propose a one-to-one constraint stable matching algorithm to maximize the sum EE of SWIPT-enabled D2D links, where the preference lists for both D2D links and CUEs will be constructed based on the results of Algorithm 2. The sum EE of non-EH D2D links will be maximized in a similar but simpler way at the end of this section.

A. Preference Lists

In order to find the most appropriate CUE for each SWIPT-enabled D2D link to share RB with such that the sum EE of all SWIPT-enabled D2D links is maximized, which is also referred to as the partner selection problem, we need to build a preference list for each SWIPT-enabled D2D link and each CUE based on the results of Algorithms 2.

Each SWIPT-enabled D2D link would prefer to share the RB of a CUE that maximizes its EE. The preference list

of D2D link i, denoted by $\Omega_i^D = \{\Omega_i^1, \Omega_i^2, \ldots, \Omega_i^k\}$, where $i \in Eha^D$, is obtained by sorting all the CUEs in S_i^D in the <mark>descending order</mark> of the EE that D2D link i can achieve when sharing their RBs. Each CUE would prefer to share its RB with a D2D link that causes the least interference to its uplink to the BS. The preference list of CUE k, denoted by $\Omega_k^C = \{\Omega_k^1, \Omega_k^2, \ldots, \Omega_k^i\}$, where $k \in S_i^D$, is constructed by sorting all the D2D links in Eha^D in the ascending order of the interference power that they cause to the BS when sharing the RB with CUE k. Therefore, we can establish the preference lists for all SWIPT-enabled D2D links and the CUEs in S_i^D.

If all the SWIPT-enabled D2D links can find their partners, the matching will be called perfect stable matching. However, sometimes due to the bad channel condition or the long D2D communication distance, some of the D2D links can only select few or even one CUE to match with for meeting the constraints, especially, for EH circuit sensitivity. Thus, such D2D links may have limited CUEs in their preference lists so as in the partner selection set S_i^D. Also, the limited CUEs may match with other D2D links they prefer based on Ω_k^C, this results in such D2D links to be unmatched. Considering the user fairness and the EE performance, we cannot let such D2D links fail to perform SWIPT. Thus, a one-to-one constraint stable matching is proposed in the next section to ensure all SWIPT-enabled D2D links can find their partners.

B. One-to-One Constraint Stable Matching Algorithm

The BS collects all the preference lists constructed as described above and runs a one-to-one constraint stable matching algorithm to ensure that each SWIPT-enabled D2D link is matched to an appropriate CUE. Since stable matching tends to favor the group that proposes to the other group [44], the algorithm lets the D2D links start proposing to the CUEs first. In each loop, the D2D links in Eh_a^D propose to their most preferred CUE one by one. If CUE k ($k \in S_i^D$) receives only one proposal, then it will select the proposing D2D link as its partner. When CUE k receives more than one proposal, if there is a proposing D2D link with only one CUE in its preference list, then CUE k will select this D2D link and reject all the others; if all the proposing D2D links have more than one CUEs on their preference lists, then CUE k will select the most preferred D2D link among the proposing D2D links according to its own preference list Ω_k^C and reject all the others.

During each loop, a D2D link will be removed from (or added to) Eha^D if it is matched to (or refused by) a CUE. At the end of each loop, all SWIPT-enabled D2D links will delete their most preferred CUE from their preference lists. In the next loop, each unmatched D2D link in Eha^D will propose to the most preferred CUE one by one in their updated preference list. The one-to-one constraint stable matching algorithm will terminate until all SWIPT-enabled D2D links have been matched to a CUE. Finally, the unmatched CUEs are gathered in Φ^R.

C. Sum EE Maximization for Non-EH D2D Links

The non-EH D2D links have been grouped in Inf^D by the prematching algorithm in Section III-A. We propose an iterative power control algorithm and a one-to-one stable

---

Algorithm 4 Constraint Stable Matching Algorithm

Input: $Eha^D, \hat{C}, \Omega_i^D, \Omega_k^C$.
Output: Φ, Φ^R.
Initialize: $\Phi = \emptyset$.

1: **while** $Eha^D \neq \emptyset$ **do**
2:     **for** $i \in Eha^D$ **do**
3:         D2D link i proposes to its most preferred CUE based on Ω_i^D.
4:         **for** $k \in S_i^D$ **do**
5:             **if** CUE k receives only one proposal from D2D link i and currently has no partner **then**
6:                 CUE k and D2D link i are matched,
7:                 $Eha^D \backslash i$, $\Phi = (i, k)$.
8:             **end if**
9:             **if** CUE k receives another proposal from D2D link i' **then**
10:                 CUE k will check Ω_i^D and $\Omega_{i'}^D$.
11:                 **if** D2D link i or i' has no more preference **then**
12:                     CUE k will match with D2D link i or i',
13:                     The matched D2D link will be removed from Eha^D, the unmatched D2D link will be added into Eha^D.
14:                 **end if**
15:                 **if** Both D2D links have other preferences **then**
16:                     CUE k will match with more preferred D2D link based on Ω_k^C,
17:                     The matched D2D link will be removed from Eha^D, the unmatched D2D link will be added into Eha^D.
18:                 **end if**
19:             **end if**
20:         **end for**
21:     **end for**
22:     All D2D links delete their most preferred CUE in Ω_i^D.
23: **end while**
24: ALL unmatched CUEs are gathered in Φ^R.

---

matching algorithm to maximize the sum EE of non-EH D2D links by matching them with the CUEs that have not been matched with any SWIPT-enabled D2D link. The difference from Algorithm 4 is that there are no constraints regarding the EH circuit sensitivity or the power splitting ratio. The optimal transmission power of non-EH D2D links i ($i \in Inf^D$) when reusing the RB of CUE k ($k \in \Phi^R$) is given by

$$P_i^{D*} = \left\{ \frac{(1+\beta')\log_2^e}{\alpha' + Q_i^{D*}} - \frac{P_k^C h_{k,i} + N_0 + N_1}{h_i^D} \right\}^+. \quad (26)$$

Proof: See Appendix D. ∎

V. COMPUTATIONAL COMPLEXITY ANALYSIS

The complexity of the prematching algorithm in Algorithm 1 is mainly determined by the number of D2D links and CUEs. Therefore, the computational complexity of Algorithm 1 is $\mathcal{O}(MN)$, where M and N are the numbers of CUEs and D2D links, respectively.

The TLEEIA algorithm employs an inner loop algorithm (i.e., Algorithm 3) and an outer loop algorithm (i.e., Algorithm 2) to solve **P1**. There are three main steps to solve **P1**. In step 1, we compute the maximum number of segments that P_i^R may belong to, denoted by $N_{\max}$. In step 2, we solve the optimization problem **P3** for given i. By solving **P3**, we obtain $N_{\max}$ power allocation and resource allocation policies, denoted by $\{P_{i,1}^D, \ldots, P_{i,j}^D, \ldots, P_{i,N_{\max}}^D\}$ and $\{\lambda_{i,1}^e, \ldots, \lambda_{i,j}^e, \ldots, \lambda_{i,N_{\max}}^e\}$, respectively, and compute the corresponding EE denoted by $\{\text{EE}_{i,1}^D, \ldots, \text{EE}_{i,j}^D, \ldots, \text{EE}_{i,N_{\max}}^D\}$. In step 3, the optimal solution of **P1** is determined by $\max_j\{\text{EE}_{i,1}^D, \ldots, \text{EE}_{i,j}^D, \ldots, \text{EE}_{i,N_{\max}}^D\}$ and is denoted by P_i^{D*}, λ_i^{e*}, EE_i^{D*}. The inner loop iterative algorithm in Algorithm 3 solves step 2. If the "while" loop of Algorithm 3 needs Δ_1 iterations to converge, the subgradient method used in Algorithm 3 needs Δ_2 iterations to converge, and the BCD method used in Algorithm 3 needs Δ_3 iterations to converge, then the update of P_a and Y need $\mathcal{O}(\Delta_3)$ operations, and the updates of each Lagrange multiplier calls $\mathcal{O}(\Delta_2)$ operations, while there are five Lagrange multipliers in Algorithm 3. Thus, the computational complexity of Algorithm 3 is $\mathcal{O}(M'N'\Delta_1 5\Delta_2\Delta_3)$, where N' and M' are the numbers of SWIPT-enabled D2D links and CUEs possible to match, respectively. The outer loop algorithm in Algorithm 2 solves step 3, where the computation times are $N_{\max}$. Therefore, the computational complexity of the TLEEIA algorithm is $N_{\max}\mathcal{O}(M'N'\Delta_1 5\Delta_2\Delta_3)$ [11], [45].

For the one-to-one constraint stable matching in Algorithm 4, due to the fact that every SWIPT-enabled D2D link has only one opportunity to propose to CUEs in its preference list, the computational complexity of Algorithm 4 is $\mathcal{O}(M'N')$ [11]. The computational complexity of the stable matching algorithm in Appendix D for non-EH D2D links is $\mathcal{O}(M''N'')$, where M'' and N'' denote the numbers of remaining CUEs and non-EH D2D links, respectively. In short-range D2D communications, since the numbers of non-EH D2D links and remaining CUEs are typically smaller than those of SWIPT-enabled D2D links and CUEs possible to match, respectively, the stable matching algorithm has lower complexity than the one-to-one constraint stable matching in Algorithm 4.[8]

VI. SIMULATION RESULTS

This section shows the simulation results of the proposed algorithms based on the piecewise linear EH model in comparison with a baseline which employs our proposed algorithms based on a linear EH model, the matching-based energy-efficient resource allocation scheme in [11], and two heuristic algorithms, including proposed matching with the maximum D2D transmission power scheme and random matching with the maximum D2D transmission power scheme. The EE is analyzed with respect to some key parameters, including the number of D2D links or CUEs and the D2D communication distance.

---

[8]The proposed algorithms are operated by the BS, without increasing the overhead for CSI acquisition or reporting as compared with the existing BS assisted D2D communications underlaying cellular network.

TABLE I
SIMULATION PARAMETERS

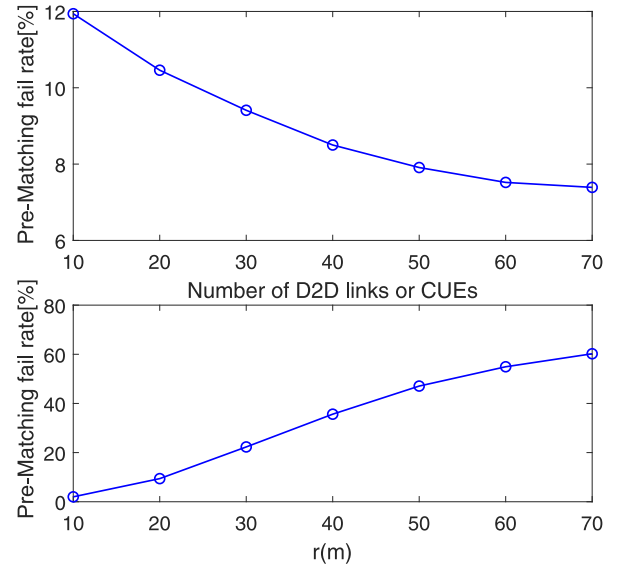| Simulation parameter	Value
Cell radius R	200 m
Number of D2D links N	10∼30
Number of CUEs M	10∼50
D2D communication distance range r	10∼60 m
Pathloss exponent α	3 [47]
Receiver power segment $[P_{th}^0, P_{th}^1, P_{th}^2, P_{th}^3]$	[10, 57368, 230.06, 100] uw
Coefficient $[k_0, k_1, k_2, k_3, k_4]$	[0, 0.3899, 0.6967, 0.1427]
Intercept $[b_0, b_1, b_2, b_3, b_4]$	[0,-1.6613,-19.1737,108.2778]
Maximum harvestable power P_{max}^{EH}	250 uw
Max transmission power for any user P_{max}	23 dBm
CUE transmission power P_k^C	23dBm
Noise power N_0, N_1	−100 dBm [11], [13], [28]
Circuit power consumption P_{cir}	20 dBm
Throughput requirement for D2D link T_{min}^D	2 bit/s/Hz
Throughput requirement for cellular link T_{min}^C	1 bit/s/Hz

Fig. 3. PMFR versus the number of D2D links (or CUEs) and D2D communication distance.

A. Parameters Initialization

The simulation parameters are listed in Table I. Without loss of generality, we assume the same number of D2D links as the number of CUEs.

B. Prematching Fail Rate

Fig. 3 shows the prematching fail rate (PMFR) versus the number of D2D links or CUEs and D2D communication distance. PMFR is defined as the ratio of the number of non-EH D2D links to the total number of D2D links as a result of the prematching algorithm. As we can see from Fig. 4, the PMFR reduces from 12% to 7.8% with users increasing from 10 to 70. Based on the proposed one-to-one constraint matching algorithm, more CUEs increase the preference list elements for each D2D link. Therefore, each D2D link has more CUEs to be matched with, which reduces the PMFR. Furthermore, the
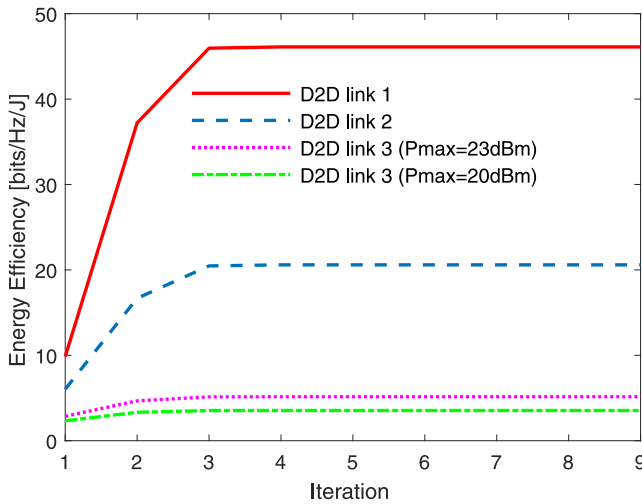
Fig. 4. Convergence of Algorithm 3.

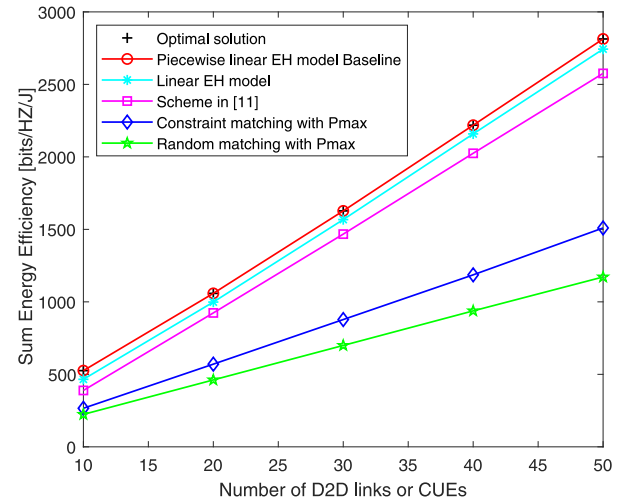Fig. 5. Sum EE versus the number of D2D links or CUEs ($r = 20$ m).

PMFR increases sharply from 2% to 61% with larger D2D communication distance range from 10 to 70 m. When the D2D communication range increases, D2D transmitters need to improve their transmission power to meet the EH constraints, once the required transmission power exceeds P_{max}, such D2D links cannot perform SWIPT which increases the number of non-EH D2D links, and we have higher PMFR. This also indicates that the PMFR is much sensitive to the D2D communication distance due to the large pathloss and rayleigh fading.

C. Convergence of Algorithm 3

Fig. 4 shows the EE per link versus the iteration step for different values of three individual D2D links. The EE of these three links converges very quickly to a unique value at step 3, and we find that the EE always converges at step 3 or step 4 for all other D2D links. It proves that this iterative algorithm is very efficient for solving the optimization problem. Also, different D2D links have different optimal EE based on the channel condition. By observing the EE of D2D link 3 with different maximum D2D transmission power limitation, the EE of D2D link 3 increases with higher maximum transmission power. Since the optimal value of P_i^D of some D2D links exceeds P_{max}, if we allow higher P_{max}, such D2D links can achieve higher EE.

D. Sum EE

In this section, we compare the sum EE of all D2D links versus the number of D2D links or CUEs, and D2D communication range for different algorithms. In Figs. 5 and 6, the "optimal solution" is obtained through the exhausting search, and the stable matching-based resource allocation algorithm of [11] (which does not consider the EE of non-EH D2D links or the optimization of the power splitting ratio) is included in comparison with our proposed algorithms under the system model as described from Sections II–IV. The piecewise linear EH model baseline is obtained by substituting the optimal P_i^D and λ_i^e under the linear EH model into the piecewise linear

EH model. Two heuristic algorithms, including constraint matching with P_{max} and random matching with P_{max} are also proposed to make comparison with our proposed algorithms in EE performance. We do not consider random power allocation in this article since the required transmission power may exceed the maximum allowed power when the channel condition is bad. If we assume random power allocation, many D2D links will not realize SWIPT which will definitely degrade the EE performance.

Fig. 5 shows the sum EE of all D2D links versus the number of D2D links or CUEs for different algorithms. As more users contribute more EE, for a fixed number of available RBs, the EE increases significantly with more D2D links and lower PMFR in Fig. 3. We can find that our proposed algorithms based on the piecewise linear EH model achieve the highest EE compared with other cases. Also, the gap between the optimal solution and the piecewise linear EH model can be definitely ignored. The difference between the EE performance of the piecewise linear EH model and baseline indicates that the linear EH model leads to resource allocation mismatches and suffers from EE performance degradation in the piecewise linear EH model. By observing the increasing gap between the piecewise linear EH model and [11], we can find that more CUEs and our proposed constraint stable matching makes it much more possible for D2D links to be matched as SWIPT-enabled D2D links and provides more EE. In Fig. 5, the sum-EE improvement of our proposed algorithms is mainly brought by the joint optimization of the D2D transmission power and the power splitting ratio of D2D receivers. We note that the sum EE gap between [11] and our proposed algorithms are not large. This is because the considered D2D communication distance (i.e., 20 m) is short, and the resultant PMFR of our proposed algorithm is low, thus the number of SWIPT-enabled D2D links in our proposed system is close to that in [11].

For the constraint matching with P_{max} and random matching with P_{max} algorithms, the power consumption issues have been totally ignored and they focus on improving the throughput of D2D links to increase EE, but this improvement cannot compensate for the loss of EE due to higher energy consumption. By the way, the random matching with the maximum
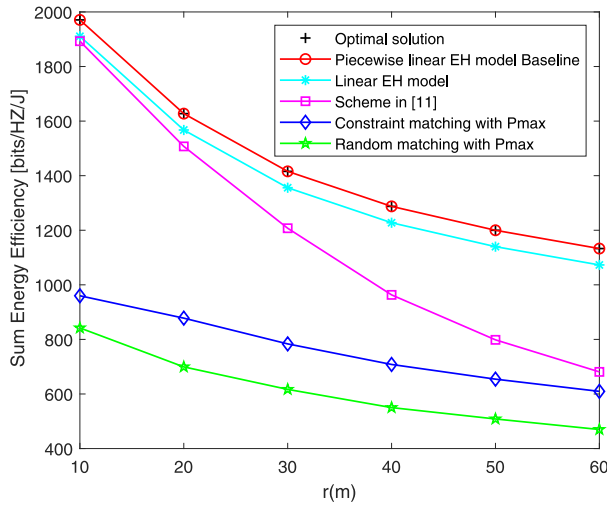
Fig. 6. Sum EE versus D2D communication distance ($N = M = 30$).

Fig. 7. Sum EE versus CUE transmission power ($N = M = 30$, $r = 25$ m).

power algorithm shows the worst EE performance, this is easy to understand that D2D links can achieve higher EE when they find better CUEs to be their partners. However, the EE performance has a limitation which depends on the number of RBs. In the system model, each CUE is allocated with one RB and each D2D link can only share the RB with one CUE, thus the number of D2D links cannot exceed the number of RBs, the sum of the EE will not increase when all RBs are allocated.

Fig. 6 shows the sum EE of D2D links versus D2D communication range r for different algorithms. Our proposed algorithms based on the piecewise linear EH model also achieve the highest EE compared with other cases. The difference between the piecewise linear EH model and the baseline also proves that the linear EH model causes resource allocation mismatches and EE performance degradation. With the increasing of D2D communication range and much lower PMFR in Fig. 3, the EE decreases sharply for all the algorithms while our proposed algorithms based on the piecewise linear EH model still shows the best EE performance, and random matching with maximum power algorithm is still the worst case. The reason for such reduction is that longer D2D communication distance requires a D2D transmitter to improve the transmission power for meeting C3 and C5, then much more energy consumption is caused. Also, the throughput of D2D links reduces due to higher pathloss. Therefore, the EE decreases with longer D2D communication distance.

Comparing the EE performance in [11] with the piecewise linear EH model, when the distance is small, e.g., below 20 m, the EE performance is quite close because the PMFR is very low with short distance, D2D links can always find their partners even we consider the practical EH model. However, there still exists a small difference due to the joint optimization of D2D transmission power and the power splitting ratio. When the distance becomes larger, more D2D links will fail to communicate in [11] due to high PMFR, which results in significant degradation of EE, but it is still higher than another two heuristic algorithms within 60 m. When the distance exceeds 60 m, the EE obtained through the scheme
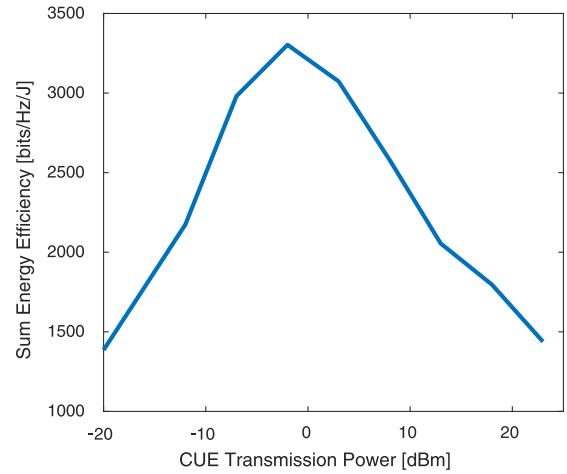
in [11] will be lower that the heuristic algorithms due to the huge reduction of the number of SWIPT-enabled D2D links. In Fig. 6, as the D2D communication distance increases, leading to a higher PMFR, the sum-EE gain of our proposed algorithm over the algorithm in [11] increases significantly. This gain is achieved by our proposed prematching and constraint stable matching algorithms in conjunction with the joint optimization of the D2D transmission power and the power splitting ratio, especially, when the D2D communication distance is long. Furthermore, we find that the EE performance of the two heuristic algorithms is relatively stable, this is because that maximum D2D transmission power is already assumed in these two algorithms, the total energy consumption remains unchanged and the lower throughput is the main reason for the reduction of EE performance. Comparing these two heuristic algorithms, constraint stable matching still shows better EE performance.

Fig. 7 plots the sum EE of D2D links in our proposed system versus the CUE transmission power. We can see that the sum EE of D2D links first increases with the CUE transmission power. This is because a higher CUE transmission power can provide more energy for D2D receivers to harvest and make it more likely for the CUE to meet the QoS requirement, resulting in a higher probability for it to be matched with a D2D link. When the CUE transmission power increases beyond a certain value (around -2 dBm in Fig. 7), the sum EE of D2D links starts to decrease. This is because the EE improvement brought by the higher harvested energy cannot compensate for the loss of EE caused by the increased interference power from co-channel CUEs.

VII. Conclusion

In this article, we have maximized the sum EE of all D2D links by optimizing the allocation of spectrum resource and transmission power in SWIPT-enabled D2D underlaid cellular networks based on a piecewise linear EH model. Specifically, we first proposed a prematching algorithm to divide D2D links into a SWIPT enable group and a non-EH group considering the EH circuit sensitivity and D2D transmission rate requirements. We then propose a one-to-one

constraint stable matching algorithm to maximize the sum EE of SWIPT-enabled D2D links, where the preference lists of CUEs and SWIPT-enabled D2D links are built based on the results of the joint optimizations of the transmission power and the power splitting ratio that maximize the EE of each SWIPT-enabled D2D link. The sum EE of the non-EH D2D links is maximized following a similar approach. The simulation results show that the sum EE is much higher with short D2D communication distance and more users, and our proposed algorithms achieve a much higher sum EE of D2D links than the existing work. In our future work, we will study the joint optimization of CUE transmission power, D2D transmission power, and the power splitting ratio to maximize the sum EE.

APPENDIX A
PROOF OF PROPOSITION 1

In order to find the convexity of the optimization problem (29), we first derive the second-order derivative of the Lagrange function $L(P_i^D, \lambda_i^e, \alpha, \beta, \gamma, \delta, \epsilon)$ with respect to λ_i^e as shown in the following equation. For simplicity, we denote this Lagrange function as L, P_i^D is regarded as a fixed value

$$\frac{\partial L^2}{\partial \lambda_i^{e2}} = \frac{-P_i^D h_i^D N_1 \log_2^e V\left((P_i^D h_i^D + V)(1 - \lambda_i^e) + N_1\right)}{\left(V(1 - \lambda_e^i) + N_1\right)^2\left((P_i^D h_i^D + V)(1 - \lambda_i^e) + N_1\right)^2}$$
$$+ \frac{-P_i^D h_i^D N_1 \log_2^e (V(1 - \lambda_i^e) + N_1)(P_i^D h_i^D + V)}{\left(V(1 - \lambda_i^e) + N_1\right)^2\left((P_i^D h_i^D + V)(1 - \lambda_i^e) + N_1\right)^2}$$
$$< 0 \qquad (27)$$

where $V = P_k^C h_{k,i} + N_0$, all the variables and constants in (27) are greater than 0, so the optimization problem is convex with respect to λ_i^e when we fix P_i^D.

Then, we fix λ_i^e and derive the second-order derivative of L with respect to P_i^D as

$$\frac{\partial L^2}{\partial P_i^{D2}} = \frac{-(1 + C)h_{i,D}^2 \log_2^e}{\left(P_i^D h_i^D + P_{k,C} h_{k,i} + N_0 + \frac{N_1}{1 - \lambda_i^e}\right)^2}$$
$$- \frac{\left(P_k^C h_k^C h_i^B \log_2^e\right)W}{U\left(P_i^D h_i^B + N_0 + N_1 + P_k^C h_k^C\right)^2} < 0 \qquad (28)$$

where $U = (P_i^D h_i^B + N_0 + N_1)^2$, $W = [(2P_i^D 2h_i^B + 2N_0 + 2N_1)h_i^B + P_k^C h_k^C h_i^B]$, all the variables and constants in (28) is greater than 0, so the optimization problem is convex with respect to P_i^D when we fix λ_i^e. Combining (27) and (28), Proposition 1 is proven.

APPENDIX B
PROOF OF THEOREM 2

We first let the first-order derivation of L with respect to λ_i^e be 0, which is formulated in (30). Then, we transform (30) into a standard quadratic equation as

$$a_1 \lambda_i^{e2} + a_2 \lambda_i^e + a_3 = 0 \qquad (29)$$

Then, we obtain the solution of (29) based on the two cases.

Case 1: If $a_2^2 - 4a_1 a_3 = 0$, there exist two equal real roots and we obtain

$$\lambda_e^{i*} = \frac{-a_2 + \sqrt{a_2^2 - 4a_1 a_3}}{2a_1} = \frac{-a_2 - \sqrt{a_2^2 - 4a_1 a_3}}{2a_1}. \qquad (30)$$

Case 2: If $a_2^2 - 4a_1 a_3 > 0$, there exist two real roots and we obtain

$$\lambda_e^{i*} = \frac{-a_2 \pm \sqrt{a_2^2 - 4a_1 a_3}}{2a_1}. \qquad (31)$$

Combining cases 1 and 2, Theorem 2 is proven.

APPENDIX C
PROOF OF THEOREM 3

We first let the first-order derivation of L with respect to $P_{i,D}$ be 0, which is formulated in (33). Then, we transform (33) into a standard cubic equation as

$$b_1 P_i^{D3} + b_2 P_i^{D2} + b_3 P_i^D + b_4 = 0 \qquad (32)$$

According to [47], we can calculate the solution of (32) based on three cases.

Case 1: If $y_N^2 > g^2$, there exists a real root and we obtain

$$P_{i,D}^* = X_N + \sqrt[3]{\frac{-y_N + \sqrt{y_N^2 - g^2}}{2b_1}} + \sqrt[3]{\frac{-y_N - \sqrt{y_N^2 - g^2}}{2b_1}}. \qquad (33)$$

Case 2: If $y_N^2 = g^2$, there exist two real roots and we obtain

$$P_i^{D*} = X_N - \theta, X_N + 2\theta. \qquad (34)$$

Case 3: If $y_N^2 < g^2$, there exist three roots and we obtain

$$P_i^{D*} = X_N + 2\theta \cos\left(\phi - \frac{2\pi n}{3}\right), \quad [n = 0, 1, 2]. \qquad (35)$$

Combining cases 1–3, Theorem 3 is proven.

APPENDIX D
EE MAXIMIZATION FOR NON-EH D2D LINKS

Similar to the optimization process of SWIPT-enabled D2D links, we first formulate the EE optimization problem for each non-EH D2D links as

$$\max_{\{P_i^D, i \in Inf^D\}} \text{EE}_i^D = \frac{\log_2\left(1 + \frac{P_i^D h_i^D}{P_k^C h_{k,i} + N_0 + N_1}\right)}{P_i^D + 2P_{\text{cir}}} \qquad (36)$$

$$\text{Subject to } 0 < P_i^D \le P_{\max} \qquad (37)$$
$$T_i^D \ge T_{\min}^D. \qquad (38)$$

Then, we employ the same nonlinear fractional programming and Lagrange dual decomposition to transform the problem in (36) into a similar Lagrange dual optimization problem which is obtained by

$$\min_{\{\alpha', \beta', \gamma' \ge 0\}} \max_{\{P_i^D, i \in Inf^D\}} L'\left(P_i^D, \alpha', \beta'\right)$$
$$= T_i^D - Q_i^D \text{EC}_i^D - \alpha'\left(P_i^D - P_{\max}\right)$$
$$+ \beta'\left(T_i^D - T_{\min}^D\right) \qquad (39)$$

where α' and β' are the Lagrange multipliers associated with (37) and (38), respectively. It is obvious to find that the optimization problem in (36) is convex with respect to $P_{i,D}$, we can easily obtain the expression of the optimal $P_{i,D}$ by using the KKT conditions as

$$P_i^{D*} = \left\{ \frac{(1+\beta')\log_2^e}{\alpha' + Q_i^D} - \frac{P_k^C h_{k,i} + N_0 + N_1}{h_i^D} \right\}^+. \quad (40)$$

The optimal P_i^D can be achieved easily by iterating (40) and updating the Lagrange multipliers until the EE of D2D link i converges to an unique value.

After the iteration, we employ a simpler one-to-one stable matching among the non-EH D2D links and remaining CUEs in Φ^R. The preference lists establishment standards are the same for both non-EH D2D links and remaining CUEs, and the matching process is still the same as we introduced above except the condition in line 11 of Algorithm 4. We do not consider the constraint in line 12 of Algorithm 4 because the requirements for non-EH D2D links are easy to meet and the preference lists of such D2D links are always full, on the other words, non-EH D2D links can always match with any of the remaining CUEs while guaranteeing the throughput requirement of the matched CUE. The sum EE of non-EH D2D links can be maximized through this simple stable matching algorithm.
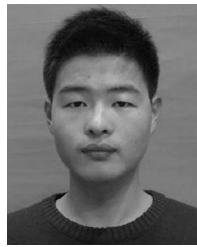
REFERENCES

[1] K. Doppler, C. B. Ribeiro, and J. Kneckt, "Advances in D2D communications: Energy efficient service and device discovery radio," in *Proc. 2nd Int. Conf. Wireless Commun. Veh. Technol. Inf. Theory Aerosp. Electron. Syst. Technol. (Wireless VITAE)*, Chennai, India, 2011, pp. 1–6.

[2] R. Q. Hu and Y. Qian, "An energy efficient and spectrum efficient wireless heterogeneous network framework for 5G systems," *IEEE Commun. Mag.*, vol. 52, no. 5, pp. 94–101, May 2014.

[3] Z. Chang, T. Ristaniemi, and Z. Niu, "Radio resource allocation for collaborative OFDMA relay networks with imperfect channel state information," *IEEE Trans. Wireless Commun.*, vol. 13, no. 5, pp. 2824–2835, May 2014.

[4] Y. Cai, Y. Ni, J. Zhang, S. Zhao, and H. Zhu, "Energy efficiency and spectrum efficiency in underlay device-to-device communications enabled cellular networks," *China Commun.*, vol. 16, no. 4, pp. 16–34, Apr. 2019.

[5] X. Liu and N. Ansari, "Green relay assisted D2D communications with dual batteries in heterogeneous cellular networks for IoT," *IEEE Internet Things J.*, vol. 4, no. 5, pp. 1707–1715, Oct. 2017.

[6] Y. Li, K. Chi, H. Chen, Z. Wang, and Y. Zhu, "Narrowband Internet of Things systems with opportunistic D2D communication," *IEEE Internet Things J.*, vol. 5, no. 3, pp. 1474–1484, Jun. 2018.

[7] L. Chettri and R. Bera, "A comprehensive survey on Internet of Things (IoT) toward 5G wireless systems," *IEEE Internet Things J.*, vol. 7, no. 1, pp. 16–32, Jan. 2020.

[8] H. Tang and Z. Ding, "Mixed mode transmission and resource allocation for D2D communication," *IEEE Trans. Wireless Commun.*, vol. 15, no. 1, pp. 162–175, Jan. 2016.

[9] R. Yin, C. Zhong, G. Yu, Z. Zhang, K. K. Wong, and X. Chen, "Joint spectrum and power allocation for D2D communications underlaying cellular networks," *IEEE Trans. Veh. Technol.*, vol. 65, no. 4, pp. 2182–2195, Apr. 2016.

[10] H. H. Esmat, M. M. Elmesalawy, and I. I. Ibrahim, "Adaptive resource sharing algorithm for device-to-device communications underlaying cellular networks," *IEEE Commun. Lett.*, vol. 20, no. 3, pp. 530–533, Mar. 2016.

[11] Z. Zhou, C. Gao, C. Xu, T. Chen, D. Zhang, and S. Mumtaz, "Energy-efficient stable matching for resource allocation in energy harvesting-based device-to-device communications," *IEEE Access*, vol. 5, pp. 15184–15196, 2017.

[12] H. Liu, K. J. Kim, K. S. Kwak, and H. V. Poor, "Power splitting-based SWIPT with decode-and-forward full-duplex relaying," *IEEE Trans. Wireless Commun.*, vol. 15, no. 11, pp. 7561–7577, Nov. 2016.

[13] Y. Xu *et al.*, "Joint beamforming and power-splitting control in downlink cooperative SWIPT NOMA systems," *IEEE Trans. Signal Process.*, vol. 65, no. 18, pp. 4874–4886, Sep. 2017.

[14] D. K. Verma, R. Y. Chang, and F. Chien, "Energy-assisted decode-and-forward for energy harvesting cooperative cognitive networks," *IEEE Trans. Cogn. Commun. Netw.*, vol. 3, no. 3, pp. 328–342, Sept. 2017.

[15] J. Tang, A. Shojaeifard, D. K. C. So, K. Wong, and N. Zhao, "Energy efficiency optimization for CoMP-SWIPT heterogeneous networks," *IEEE Trans. Commun.*, vol. 66, no. 12, pp. 6368–6383, Dec. 2018.

[16] Y. Xu, G. Li, Y. Yang, M. Liu, and G. Gui, "Robust resource allocation and power splitting in SWIPT enabled heterogeneous networks: A robust minimax approach," *IEEE Internet Things J.*, vol. 6, no. 6, pp. 10799–10811, Dec. 2019.

[17] O. B. Akan, O. Cetinkaya, C. Koca, and M. Ozger, "Internet of hybrid energy harvesting things," *IEEE Internet Things J.*, vol. 5, no. 2, pp. 736–746, Apr. 2018.

[18] F. Deng, X. Yue, X. Fan, S. Guan, Y. Xu, and J. Chen, "Multisource energy harvesting system for a wireless sensor network node in the field environment," *IEEE Internet Things J.*, vol. 6, no. 1, pp. 918–927, Feb. 2019.

[19] F. Deng, H. Qiu, J. Chen, L. Wang, and B. Wang, "Wearable thermoelectric power generators combined with flexible super capacitor for low-power human diagnosis devices," *IEEE Trans. Ind. Electron.*, vol. 64, no. 2, pp. 1477–1485, Feb. 2017.

[20] Z. Kuang, G. Liu, G. Li, and X. Deng, "Energy efficient resource allocation algorithm in energy harvesting-based D2D heterogeneous networks," *IEEE Internet Things J.*, vol. 6, no. 1, pp. 557–567, Feb. 2019.

[21] A. H. Sakr and E. Hossain, "Cognitive and energy harvesting-based D2D communication in cellular networks: Stochastic geometry modeling and analysis," *IEEE Trans. Commun.*, vol. 63, no. 5, pp. 1867–1880, May 2015.

[22] Y. Chen, K. T. Sabnis, and R. A. Abd-Alhameed, "New formula for conversion efficiency of RF EH and its wireless applications," *IEEE Trans. Veh. Technol.*, vol. 65, no. 11, pp. 9410–9414, Nov. 2016.

[23] Y. Huo, X. Dong, T. Lu, W. Xu, and M. Yuen, "Distributed and multilayer UAV networks for next-generation wireless communication and power transfer: A feasibility study," *IEEE Internet Things J.*, vol. 6, no. 4, pp. 7103–7115, Aug. 2019.

[24] M. Zhao, Q. Shi, and M. Zhao, "Efficiency maximization for UAV-enabled mobile relaying systems with laser charging," *IEEE Trans. Wireless Commun.*, early access, Feb. 12, 2020, doi: 10.1109/TWC.2020.2971987.

[25] J. Huang, C. Xing, and C. Wang, "Simultaneous wireless information and power transfer: Technologies, applications, and research challenges," *IEEE Commun. Mag.*, vol. 55, no. 11, pp. 26–32, Sep. 2017.

[26] R. I. Ansari, S. A. Hassan, and C. Chrysostomou, "A SWIPT-based device-to-device cooperative network," in *Proc. 24th Int. Conf. Telecommun. (ICT)*, 2017, pp. 1–5.

[27] D. Lim, J. Kang, C. Chun, and H. Kim, "Joint transmit power and time-switching control for device-to-device communications in SWIPT cellular networks," *IEEE Commun. Lett.*, vol. 23, no. 2, pp. 322–325, Feb. 2019.

[28] D. Lim, J. Kang, and H. Kim, "Adaptive power control for D2D communications in downlink SWIPT networks with partial CSI," *IEEE Wireless Commun. Lett.*, vol. 8, no. 5, pp. 1333–1336, Oct. 2019.

[29] L. Shi, Y. Ye, R. Q. Hu, and H. Zhang, "Energy efficiency maximization for SWIPT enabled two-way DF relaying," *IEEE Signal Process. Lett.*, vol. 26, no. 5, pp. 755–759, May 2019.

[30] G. Lu, L. Shi, and Y. Ye, "Maximum throughput of TS/PS scheme in an AF relaying network with non-linear energy harvester," *IEEE Access*, vol. 6, pp. 26617–26625, 2018.

[31] P. Sun, K. G. Shin, H. Zhang, and L. He, "Transmit power control for D2D-underlaid cellular networks based on statistical features," *IEEE Trans. Veh. Technol.*, vol. 66, no. 5, pp. 4110–4119, May 2017.

[32] D. Burghal and A. F. Molisch, "Efficient channel state information acquisition for device-to-device networks," *IEEE Trans. Wireless Commun.*, vol. 15, no. 2, pp. 965–979, Feb. 2016.

[33] H. H. Yang, J. Lee, and T. Q. S. Quek, "Heterogeneous cellular network with energy harvesting-based D2D communication," *IEEE Trans. Wireless Commun.*, vol. 15, no. 2, pp. 1406–1419, Feb. 2016.

[34] J. Hu, W. Heng, X. Li, and J. Wu, "Energy-efficient resource reuse scheme for D2D communications underlaying cellular networks," *IEEE Commun. Lett.*, vol. 21, no. 9, pp. 2097–2100, Sep. 2017.

[35] S. Dominic and L. Jacob, "Distributed resource allocation for D2D communications underlaying cellular networks in time-varying environment," *IEEE Commun. Lett.*, vol. 22, no. 2, pp. 388–391, Feb. 2018.

[36] M. R. Mili, P. Tehrani, and M. Bennis, "Energy-efficient power allocation in OFDMA D2D communication by multi objective optimization," *IEEE Wireless Commun. Lett.*, vol. 5, no. 6, pp. 668–671, Dec. 2016.

[37] A. Abrardo and M. Moretti, "Distributed power allocation for D2D communications underlaying/overlaying OFDMA cellular networks," *IEEE Trans. Wireless Commun.*, vol. 16, no. 3, pp. 1466–1479, Mar. 2017.

[38] Y. Yuan, T. Yang, H. Feng, and B. Hu, "An iterative matching-Stackelberg game model for channel-power allocation in D2D underlaid cellular networks," *IEEE Trans. Wireless Commun.*, vol. 17, no. 11, pp. 7456–7471, Nov. 2018.

[39] K. Xiong, Y. Zhang, Y. Chen, and X. Di, "Power splitting based SWIPT in network-coded two-way networks with data rate fairness: An information-theoretic perspective," *China Commun.*, vol. 13, no. 12, pp. 107–119, Dec. 2016.

[40] L. Shi, L. Zhao, K. Liang, X. Chu, G. Wu, and H. H. Chen, "Profit maximization in wireless powered communications with improved non-linear energy conversion and storage efficiencies," in *Proc. IEEE Int. Conf. Commun.*, May 2017, pp. 1–6.

[41] E. Boshkovska, D. W. K. Ng, N. Zlatanov, and R. Schober, "Practical non-linear energy harvesting model and resource allocation for SWIPT systems," *IEEE Commun. Lett.*, vol. 19, no. 12, pp. 2082–2085, Dec. 2015.

[42] W. Dinkelbach, "On nonlinear fractional programming," *Manag. Sci.*, vol. 13, no. 7, pp. 492–498, Mar. 1967.

[43] D. T. Ngo, S. Khakurel, and T. Le-Ngoc, "Joint subchannel assignment and power allocation for OFDMA femtocell networks," *IEEE Trans. Wireless Commun.*, vol. 13, no. 1, pp. 342–355, Jan. 2014.

[44] D. Gale and L. S. Shapley, "College admissions and the stability of marriage," *Amer. Math. Month.*, vol. 120, no. 5, pp. 386–391, 1962.

[45] H. Zhang, C. Jiang, N. C. Beaulieu, X. Chu, X. Wen, and M. Tao, "Resource allocation in spectrum-sharing OFDMA femtocells with heterogeneous services," *IEEE Trans. Commun.*, vol. 62, no. 7, pp. 2366–2377, Jul. 2014.

[46] K. Haneda *et al.*, "Indoor 5G 3GPP-like channel models for office and shopping mall environments," in *Proc. IEEE Int. Conf. Commun. Workshops (ICC)*, 2016, pp. 694–699.

[47] Y. Ye, R. Q. Hu, G. Lu, and L. Shi, "Enhance latency-constrained computation in MEC networks using uplink NOMA," *IEEE Trans. Commun.*, vol. 68, no. 4, pp. 2409–2425, Apr. 2020, doi: 10.1109/TCOMM.2020.2969666.

Yinghui Ye received the M.S. degree in communication and information system from Xi'an University of Posts and Telecommunications, Xi'an, China, in 2016. He is currently pursuing the Ph.D. degree with the Department of Electrical and Computer Engineering, Utah State University, Logan, UT, USA, under the supervision of Prof. R. Q. Hu.

He joined the Department of Communication and Information Engineering, Xi'an University of Posts and Telecommunications in 2020. He has authored/coauthored more than 20 technical articles in the IEEE TRANSACTIONS, journals, letters, and conferences. His research interests include cognitive radio networks, relaying networks, and wireless energy harvesting.

Mr. Ye received the Exemplary Reviewer Award from IEEE WIRELESS COMMUNICATIONS LETTERS in 2019. He is also a Reviewer of multiple international journals, such as the IEEE JOURNAL ON SELECTED AREAS IN COMMUNICATIONS, the IEEE TRANSACTIONS ON COMMUNICATIONS, the IEEE TRANSACTIONS ON WIRELESS COMMUNICATIONS, and the IEEE TRANSACTIONS ON VEHICULAR TECHNOLOGY. He served as a TPC Member of IEEE VTC-FALL 2019 and IEEE ICCT 2019.

Xiaoli Chu (Senior Member, IEEE) received the B.Eng. degree in electronic and information engineering from Xi'an Jiao Tong University, Xi'an, China, in 2001, and the Ph.D. degree in electrical and electronic engineering from Hong Kong University of Science and Technology, Hong Kong, in 2005.

She is a Professor with the Department of Electronic and Electrical Engineering, University of Sheffield, Sheffield, U.K. From 2005 to 2012, she was with the Centre for Telecommunications Research, King's College London, London, U.K. She has coauthored over 150 peer-reviewed journal and conference papers. She has coauthored/co-edited the books *Fog-Enabled Intelligent IoT Systems* (Springer, 2020), *Ultra Dense Networks for 5G and Beyond* (Wiley, 2019), *Heterogeneous Cellular Networks: Theory, Simulation and Deployment* (Cambridge University Press, 2013), and *4G Femtocells: Resource Allocation and Interference Management* (Springer, 2013).

Prof. Chu received the IEEE Communications Letters Exemplary Editor Award in 2018. She was a co-recipient of the IEEE Communications Society 2017 Young Author Best Paper Award. She was the Co-Chair of Wireless Communications Symposium for IEEE ICC 2015, Workshop Co-Chair for IEEE GreenCom 2013, and has co-organized eight workshops at IEEE ICC, GLOBECOM, WCNC, and PIMRC. She is a Senior Editor of IEEE WIRELESS COMMUNICATIONS LETTERS and an Editor of IEEE COMMUNICATIONS LETTERS.
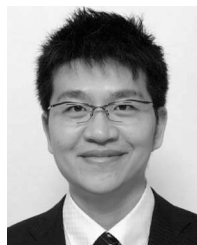
Mianxiong Dong (Member, IEEE) received the B.S., M.S., and Ph.D. degrees in computer science and engineering from the University of Aizu, Aizuwakamatsu, Japan, in 2006, 2008, and 2013, respectively.

He became the youngest ever Professor with the Muroran Institute of Technology, Muroran, Japan, where he currently serves as the Vice President. He was a JSPS Research Fellow with the School of Computer Science and Engineering, University of Aizu and a Visiting Scholar with the BBCR Group, University of Waterloo, Waterloo, ON, Canada, supported by the JSPS Excellent Young Researcher Overseas Visit Program from April 2010 to August 2011.

Dr. Dong was a recipient of the IEEE TCSC Early Career Award in 2016, the IEEE SCSTC Outstanding Young Researcher Award in 2017, the 12th IEEE ComSoc Asia–Pacific Young Researcher Award in 2017, the Funai Research Award in 2018, and the NISTEP Researcher 2018 (one of only 11 people in Japan) in recognition of significant contributions in science and technology. He is a Clarivate Analytics Highly Cited Researcher (Web of Science) in 2019.

Haohang Yang (Graduate Student Member, IEEE) received the B.Eng. degree from the Jinling Institute of Technology, Nanjing, China, and De Montfort University, Leicester, U.K., in 2016, and the M.S. degree in wireless communication systems from the University of Sheffield, Sheffield, U.K., in 2017, where he is currently pursuing the Ph.D. degree.

He attended the European commission decade project with Ranplan, Barcelona, Spain, in 2018. His current research interests include relaying networks and wireless energy harvesting.